A Novel Method for Controlling the Sublayer Microstructure of an Ultrafiltration Membrane: The Preparation of the PSF–Fe_3O_4 Ultrafiltration Membrane in a Parallel Magnetic Field

Zheng-Qing Huang, Long Chen, Kun Chen, Zhi Zhang, Hong-Tao Xu

School of Chemical and Environmental Engineering, Hubei University of Technology, Wuhan 430068, People's Republic of China

Received 1 April 2009; accepted 30 January 2010
DOI 10.1002/app.32191
Published online 1 April 2010 in Wiley InterScience (www.interscience.wiley.com).

ABSTRACT: It is very important to control the substructure of a membrane prepared by the phase inversion process. This article reports a novel method to control the substructure of ultrafiltration (UF) membrane by the combined effect of a magnetic filler and a parallel magnetic field. A series of polysulfone (PSF)–ferrosoferric oxide (Fe_3O_4) UF membranes with different amounts of Fe_3O_4 were prepared in a parallel magnetic field from suspensions, using the phase inversion process. The suspensions consisted of PSF, *N*,*N*-dimethylacetamide, poly(vinylpyrrolidone), and Fe_3O_4. Magnetic Fe_3O_4 particles in a casting solution are expected to arrange along the direction of a magnetic field during the membrane formation. This kind of oriented arrangement can gradually change the cross-sectional microstructure of a membrane from normal finger-like macrovoids perpendicular to the membrane surface into macrovoids parallel to the membrane surface, with increasing Fe_3O_4 content. As a result, a novel membrane with "lamellar macrovoids" (parallel to the membrane surface) in the sublayer was prepared as the Fe_3O_4 content reached 70 wt %. Furthermore, the membrane with 70 wt % Fe_3O_4 not only had the best flux and rejection but also had a good antipressure ability. The formation mechanism of novel microstructure of the sublayer in the UF membrane is also discussed. J Appl Polym Sci 117: 1960–1968, 2010

Key words: polysulfone; ferrosoferric oxide; magnetic field; membrane structure; ultrafiltration membrane

INTRODUCTION

Ultrafiltration (UF) membranes are mainly produced by the phase inversion process via immersion precipitation. In this technique, a homogeneous polymer solution containing polymer and adequate solvent with or without an additive is cast onto a glass plate and immersed in a coagulation bath (in some cases after a short period of solvent evaporation). The diffusive exchange of solvent and nonsolvent introduces liquid–liquid phase separation, and the successive solidification of the phase-separated solution leads to a porous, asymmetric structure.[1,2] The morphology and performance of membranes depend strongly on the thermodynamics as well as kinetics of the phase inversion process.[3] It is well known that the microstructures of membranes can be adjusted by the composition of the polymer solution (additives, etc.), the solvent evaporation temperature and evaporation time, and the nature and temperature of the gelation media.[4] However, there are two main types of asymmetric UF membranes available on the market, either with a selective thin microporous top layer on a thicker macroporous globular or spongy sublayer or with large voids and/or finger-like cavities beneath the microporous top layer. Both of these asymmetric UF membranes have disadvantages; the membrane with a spongy sublayer has a low flux, and the membrane with finger-like cavities perpendicular to the membrane surface is susceptible to compaction and mechanical failure.[5,6] According to the literature,[7–9] UF membrane compaction is related to the membrane substructure. The membrane with a high flux and no leakage at high pressure has a wide application, such as acting as a support for gas membranes. Therefore, it is very important to control the substructure of a membrane prepared by the phase inversion process.

Organic–inorganic hybrid (mixed matrix) membranes prepared by the addition of a mineral filler to polymer membranes exhibit characteristics of both ceramic and organic polymers. Polysulfone (PSF) is one of the most extensively applied UF

Correspondence to: Z.-Q. Huang (huangzq18@126.com).
Contract grant sponsor: National Natural Science Foundation of China; contract grant number: 20476023.
Contract grant sponsor: Education Department of Hubei Province; contract grant number: 2001A02003.

membrane materials in industry area for mechanical strength, compaction resistance, chemical stability, and thermal resistance. Over past few years, PSF–inorganic hybrid UF membranes have received much attention. In studies of PSF–inorganic hybrid UF membranes, the mineral fillers mainly used are zirconia,[10,11] aerosil,[12,13] TiO_2,[14–16] and ferrosoferric oxide (Fe_3O_4).[17,18] Fe_3O_4 has excellent thermal and chemical stability and good magnetic performance. The performance of organic–inorganic hybrid membranes with Fe_3O_4 filler has a special relation to an external magnetic field. Jian et al.[17] investigated the effect of a magnetic field on the performance of PSF–Fe_3O_4 UF membrane and observed an interesting phenomenon: the rejection to lysozyme of a PSF–Fe_3O_4 UF membrane at a transmembrane pressure of 0.10 MPa can change from 88 to 3% as the magnetic intensity of an external magnetic field increases from 0.0 to 0.5 T, but the rejection to lysozyme of a PSF UF membrane is invariable under the same conditions. We also found that the magnetized polyacrylonitrile (PAN)–Fe_3O_4 membrane had a higher flux than the corresponding nonmagnetized membrane in the UF of pig blood solution.[19] Magnetic Fe_3O_4 particles in a casting solution are expected to arrange along the direction of a magnetic field during the membrane formation. The microstructure and the performance of PAN–Fe_3O_4 hybrid membranes prepared in an orthogonal magnetic field were investigated in our earlier work.[20] However, the effect of a parallel magnetic field on a Fe_3O_4 hybrid membrane has not yet reported so far. The preparation of PSF–Fe_3O_4 UF membranes in a parallel magnetic field was investigated in this article. The PSF–Fe_3O_4 UF membrane with a novel substructure can be prepared in a parallel magnetic field. An aqueous solution of BSA was chosen to estimate the separation performance of UF membranes prepared in this work for two reasons. First, proteins purification and separation have been widely studied because of their important properties and applications in biotechnology and food industries. UF has the potential to meet this application because of its inherent "mild" operating conditions (i.e., relatively low temperatures, low pressures, no phase changes, or chemical additives), its economical advantages, compared with other separation techniques, and the ease of scale up.[21,22] However, the membrane fouling is one of the primary obstacles for the application of UF in the proteins purification and separation. Second, some proteins such as egg albumin and BSA are usually used as standard substances to evaluate the selectivity of industrial UF membranes, because BSA is a cheap substance and has a sharp molecular weight distribution. Furthermore, the apparatus is available in the common place, and this method is also simple and reliable.

TABLE I
Composition of Casting Solution and the Content of Fe_3O_4 Particles

Membranes	DMAC (mL)	PVP (g)	PSF (g)	Fe_3O_4 (g)	Fe_3O_4/(PSF+Fe_3O_4) (%)
1	100	5.0	28.0	0.0	0.0
2	100	5.0	28.0	3.1	10.0
3	100	5.0	28.0	7.0	20.0
4	100	5.0	28.0	12.0	30.0
5	100	5.0	28.0	18.7	40.0
6	100	5.0	28.0	28.0	50.0
7	100	5.0	28.0	42.0	60.0
8	100	5.0	28.0	65.3	70.0

MATERIALS AND METHODS

Materials

Polysulfone (PSF, $[\eta] = 0.62$) was purchased from the ShuGuang Chemical Plant in Shanghai. *N*,*N*-Dimethylacetamide (DMAC) and Fe_3O_4 were of analytical grade. Ferrosoferric oxide was used after being sieved with a 0.08-mm sieve. Polyvinylpyrrolidone (PVP 30k) and albumin bovine V (BSA from Roche, Mr 68,000) from bovine serum were used in these experiments. The demineralized water with an electric conductivity of 5 μs cm^{-1} was produced using a reverse osmosis system.

Membrane preparation

Poly(vinylpyrrolidone) was used as an additive and was added to DMAC to form a solution. Following complete dissolution of the additive, Fe_3O_4 and PSF were added to the solution. The composition of the casting solution and the content of Fe_3O_4 particles in the membranes are detailed in Table I. The solution was then shaken for 24 h at 60°C to promote the solution of PSF and prevent Fe_3O_4 particles from aggregating. After homogeneous suspension was cooled to room temperature, the membranes were cast in air (25°C ± 1°C, humidity 30–40%) on a glass plate with a glass knife. After a 5-s delay, the glass plate was placed into an open vessel with a magnetic field whose direction was parallel to the glass plate. Following a delay of 25 s, demineralized water was then poured into the vessel to cover the glass plate. The coating was taken out after 15 min and then immersed in demineralized water for 24 h.

Characterization of membranes

The cross-sectional structure of the membranes was observed using scanning electron microscopy (SEM) on a JSM-5610LV scanning microscope. The surface structure of the membranes was observed using a field emission energy filter electron microscope (JEM-2010FEF).

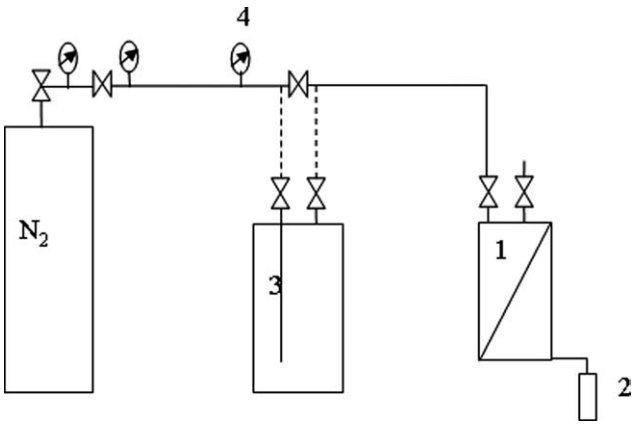

Figure 1 Schematic drawing of the dead-end UF process. 1, Dead-end UF cell [effective volume of 2.2 L, effective membrane area of 63.6 (cm^2)]; 2, permeate; 3, pure water reservoir; 4, gas pressure meter (0–600 kPa).

Membrane separation procedure

The initial pure water flux (J_0) was examined with a dead-end filtration equipment (Fig. 1) at 25°C ± 1°C room temperature, with a transmembrane pressure of 100 kPa. An aqueous solution of BSA with a concentration of 150 mg/L and a volume of 1.97 L (30 mL as the feed) was added to the aforementioned filtration equipment (without the connection of pure water reservoir). After immersion of 5 min, the pressure was adjusted to 100 kPa. The first 30 mL of permeate (measured by a 50-mL graduated cylinder) was immediately collected for determination of the initial rejection, and the test was ended when the rest volume of permeate reached 900 mL (measured by a 1000-mL graduated cylinder). The initial rejection to BSA (R_0) was determined using an ultraviolet/visible (UV) spectrophotometer (Cary 50, Varian Australia Pty) at 280 nm. Afterward, the used membrane was flushed five times with 300 mL of fresh demineralized water. The pure water flux (J_1) from the fouling membranes was then measured at a different pressure. Finally, the rejection of membrane (R_1) was measured again with the same procedure as the measurement of initial rejection.

The pure water flux of a membrane (J_0 or J_1) was calculated using the following equation:

$$J = \frac{V}{A \cdot t}, \tag{1}$$

where J is the pure water flux (L m^{-2} h^{-1}), V is the permeate volume collected (L), A is the membrane area (m^2), and t is the sampling time (h).

The membrane rejection (R_0 or R_1) was calculated using the following equation:

$$R_0(\%) = \left(1 - \frac{C_p}{C_f}\right) \times 100, \tag{2}$$

where C_p and C_f are the concentrations of the solute in permeate and feed solutions, respectively.

The relative flux of a membrane (J_r) was calculated using the following equation:

$$J_r = \frac{J_1}{J_0} \times 100. \tag{3}$$

RESULTS AND DISCUSSION

Cross-sectional structure of membranes

To understand the effect of the Fe_3O_4 content (Table I) on the cross-sectional structures, the cross sections along and across the direction of magnetic field were investigated using SEM. Some micrographs of cross sections in the two directions are displayed in Figure 2.

As seen in Figure 2 (micrographs 1C and 1A, 2C and 2A), there is no difference in the substructure between the two cross sections from a membrane with Fe_3O_4 below 20 wt %. These membranes have similar finger-like macrovoids in the sublayer. When the Fe_3O_4 content in a membrane reaches 40 wt %, the cross section along the direction of the magnetic field (micrograph 4A in Fig. 2) is quite different from the cross section perpendicular to the direction of a magnetic field (micrograph 4C in Fig. 2). The oriented alignment of magnetic Fe_3O_4 particles along the magnetic field destroys the microstructure of the perpendicular section, and the sublayer (micrograph 4A in Fig. 2) has a composite microstructure containing the finger-like macrovoids across the membrane surface and some grooves along the direction of the oriented alignment of magnetic Fe_3O_4 particles. The micrographs from 5A to 7A in Figure 2 show that the effect of the oriented alignment of magnetic Fe_3O_4 particles on the microstructure of the sublayer becomes stronger with increasing Fe_3O_4 content in the membranes. The finger-like macrovoids across the membrane surface can be found in the micrograph 5A in Figure 2 but disappear in micrograph 7A. This result indicates that the microstructure of the cross section changes with the Fe_3O_4 content in the membranes. The change of microstructure in the sublayers from another cross section can also be observed in Figure 2. The shallow and long finger-like macrovoids in micrograph 1C of Figure 2 gradually become deeper and shorter tear-shaped macrovoids in micrograph 7C with the increase of Fe_3O_4 content from 10 to 70 wt %.

The results from Figure 2 indicate that the oriented alignment of magnetic Fe_3O_4 particles in a magnetic field will change the finger-like macrovoids across the membrane surface into macrovoids along the membrane surface with increase of Fe_3O_4

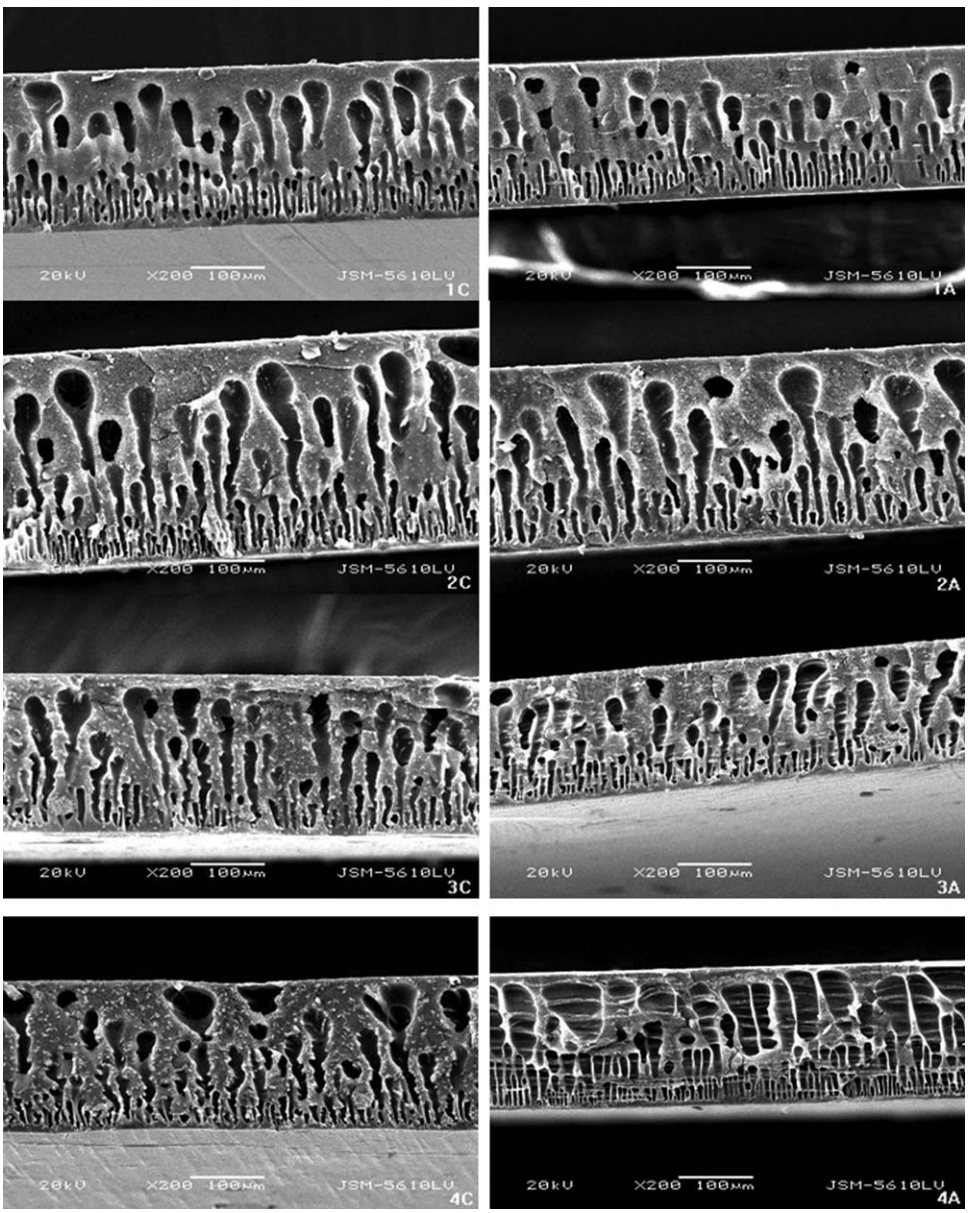

Figure 2 Cross-sectional micrographs of membranes: "A" represents the cross section along the direction of the magnetic field, and "C" represents the cross section across (perpendicular to) the direction of magnetic field; numbers from "1" to "7" represent the membranes with different Fe_3O_4 concentrations from "10.0" to "70.0 wt %."

content, and a novel membrane with "lamellar macrovoids" (parallel to the membrane surface) in the sublayer can be prepared (micrograph 7A of Fig. 2).

Formation mechanism of novel microstructure of the sublayer

Macrovoids are often present in systems exhibiting instantaneous demixing. The macrovoid formation is believed to be a result of the liquid–liquid demixing process, where the nuclei of the polymer-poor phase are also responsible for macrovoid formation. Growth of the nuclei takes place because of the diffusional flow of solvent from the surrounding polymer solution. Most of the macrovoids start to develop just beneath the top layer, initiated by some of the nuclei, which are formed directly beneath the top layer.[23] McKelvey and Koros[24] developed the hypothesis of macrovoid growth and suppression, based on the study of the dynamics of phase inversion presented by McHugh and Tsay.[25] This hypothesis explains well the presented experimental results. The authors postulate that macrovoids are initiated by nucleation of the polymer-lean phase just beneath the skin layer, as suggested previously by Smolders et al.[26] Aerts et al.[12] investigated the effect of the addition of aerosil on the membrane formation process and described the formation of macrovoids in

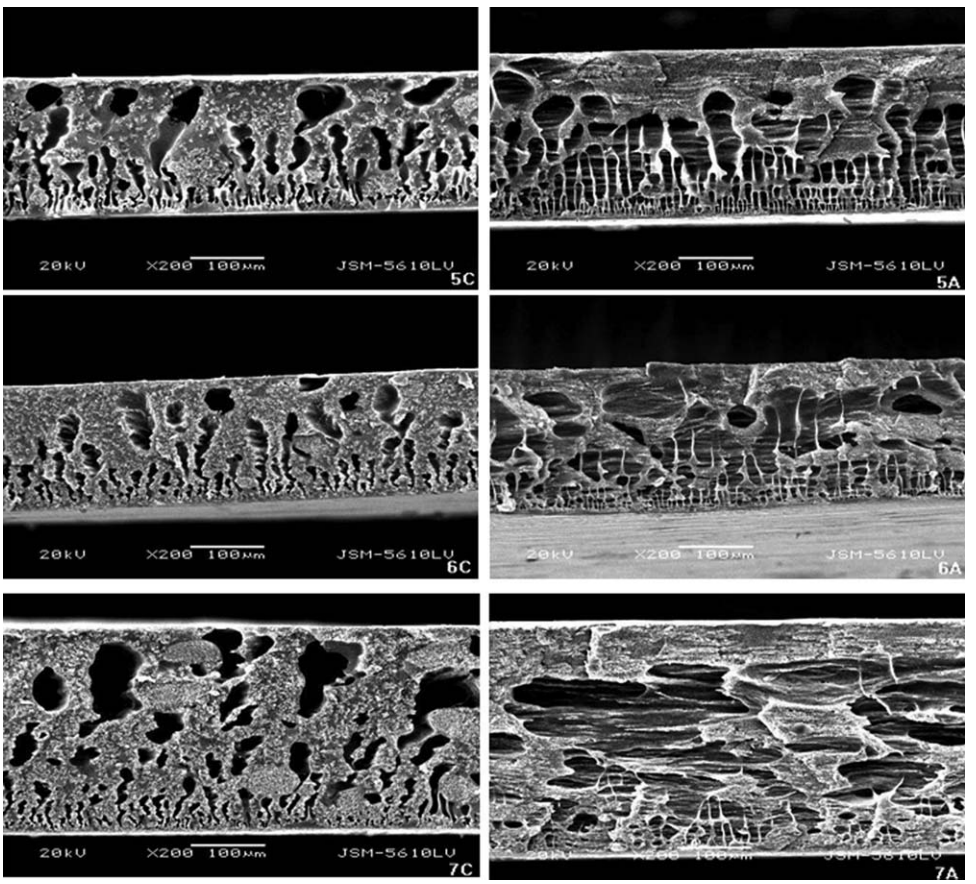

Figure 2 (*Continued from the previous page*)

an organomineral membrane system by the hypothesis presented by McKelvey and Koros.[24]

Our systems exhibit instantaneous liquid–liquid demixing because of a high mutual affinity between DMAc and water. Some droplets of the polymer-poor phase are first formed beneath the top layer. When the Fe_3O_4 content is low, the density of alignment-oriented Fe_3O_4 particles is low, and the effect of filler on the solvent/nonsolvent diffusion can be ignored. The nonsolvent flux of inward diffusion is relatively high and the diffusion front moves ahead of the precipitation front.[12] As a result, large concentration gradients are formed in the casting solution that generates osmotic pressure in the nuclei. In this situation, the growth of macrovoids continues until the precipitation occurs. Finally, ordinary finger-like macrovoid structures can be observed in both cross sections in a membrane with less than 30 wt % Fe_3O_4 (1C and 1A, 2A and 2C, and 3A and 3C in Fig. 2).

When the Fe_3O_4 content reaches 40 wt %, the density of alignment-oriented Fe_3O_4 particles becomes higher and the effect of filler on the solvent/nonsolvent diffusion cannot be ignored. The alignment-oriented Fe_3O_4 particles in front of the droplets of the polymer-poor phase look like "rods" and "alignment-oriented rods" along the direction of the magnetic field can obviously hinder forward diffusion. The diffusion of solvent/nonsolvent has to pass by "the rods" into nuclei. In this case, nuclei will grow along two directions—parallel and perpendicular—to the magnetic field. Some grooves in the macrovoids of microphoto 4A in Figure 2 indicate the growth of nuclei along the direction of the magnetic field. Furthermore, the finger-like macrovoids of microphotos 4A and 4C in Figure 2 also indicate the growth of nuclei perpendicular to the magnetic field.

Aerts et al.[12] concluded that the addition of 2 vol % aerosil slowed down the movement of the demixing front and suppressed the initiation and growth of macrovoids. When the aerosil content was increased from 1 to 2 vol %, the suspension became very viscous and slowed down the diffusion of the nonsolvent. Consequently, the diffusion front was not ahead of the precipitation front. This kinetic effect induced shallow concentration profiles in the casting suspension. Only a few diffusion fringes were observed, and a smaller osmotic pressure was built up in the growing macrovoids. The front side of the growing macrovoid was in contact with a highly viscous suspension that precipitated at a lower nonsolvent concentration. In our system, the

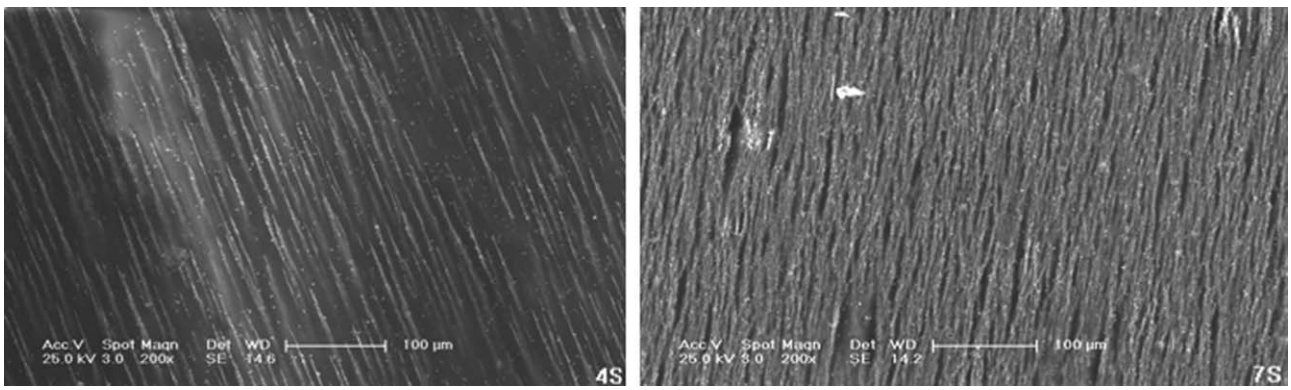

Figure 3 Surface micrographs of membranes with 40 wt % Fe_3O_4 (4S) and 70 wt % Fe_3O_4 (7S).

macrovoids of micrographs from 4C to 7C in Figure 2 gradually become shorter and fewer, when the Fe_3O_4 content is changed from 40 to 70 wt %. This result is in agreement with the conclusion of Aerts et al.[12]

In addition, an external magnetic field was applied before casting solutions were immersed into a gelation medium in this article. All Fe_3O_4 particles like small balls in casting solutions are obliged to move with a little casting solution and form "alignment-oriented round rods" along the direction of the magnetic field. When the Fe_3O_4 content is changed from 40 to 70 wt %, "alignment-oriented rods" along the direction of the magnetic field become dense (as seen in the micrographs 4S and 7S of Fig. 3). On the one hand, denser "alignment-oriented rods" will form more grooves on the surface, which will result in an increase of surface roughness. On the other hand, the forward diffusion under the surface will further be hindered by those dense "alignment-oriented rods" along the direction of the magnetic field. The growth of nuclei perpendicular to the direction of magnetic field becomes more difficult with the increase of Fe_3O_4 content from 50 to 70 wt %. Finally, no macrovoid across the direction of magnetic field can be observed from the microphoto 7A in Figure 2. However, there is still a smaller osmotic pressure exists in those nuclei of the polymer-poor phase. Those nuclei are obliged to grow along the direction of magnetic field because of the hindrance of dense "alignment-oriented rods." As a result, macrovoids growing along the direction of magnetic field can be obtained in microphoto 7A of Figure 2. In the meantime, the change of growth direction of nuclei also influences the stability of the polymer solution in front of the nuclei, and some new nuclei will form and grow along the direction of the magnetic field. Finally, the macrovoids with a "lamellar" structure can be obtained in microphoto 7A of Figure 2, and the single and dark macrovoids in microphoto 7C of Figure 2 can also be observed. Darker macrovoids are deeper. These results indicate that the magnetic field can change the growth direction of nuclei by dense alignment-oriented Fe_3O_4 particles.

Performance of membranes

Table II shows the pure water fluxes of membranes (J_0) with different Fe_3O_4 content. When the Fe_3O_4 content is less than 40 wt %, the pure water flux of the membranes increases slightly with the increase

TABLE II
Comparison of Separation Performance Between Membranes Prepared in a Parallel Magnetic Field (This Work) and Membranes Prepared Without a Magnetic Field (Ref. 18)

Fe_3O_4 (wt %)	J_0 (L m^{-2} h^{-1})	R_0 (%)	R_1 (%)	J_1 (L m^{-2} h^{-1})	J_r (%)
0 (–)[a]	6.9 (–)	90.9 (–)	94.8 (–)	6.8 (–)	98.5 (–)
10 (–)	8.1 (–)	85.4 (–)	91.3 (–)	7.5 (–)	92.3 (–)
20 (20.4)	13.4 (18.6)	77.2 (63.9)	79.5 (86.2)	12.5 (8.0)	93.3 (43.1)
30 (28.6)	12.5 (8.0)	96.0 (75.3)	83.3 (89.1)	10.9 (6.1)	87.2 (76.7)
40 (37.5)	20.3 (32.0)	93.1 (85.5)	81.1 (94.8)	17.2 (16.7)	84.7 (52.4)
50 (47.4)	19.3 (35.9)	68.6 (87.9)	84.8 (97.7)	13.5 (23.1)	69.9 (64.3)
60 (58.3)	37.4 (208.2)	97.0 (90.2)	91.3 (97.2)	30.7 (129.1)	82.1 (62.0)
70 (70.6)	68.6 (373.8)	96.9 (82.1)	98.7 (92.9)	39.5 (243.0)	57.6 (65.0)
– (84.4)	– (398.7)	– (50.8)	– (82.9)	– (120.2)	– (30.1)

[a] Data in the parenthesis from Ref. 18.

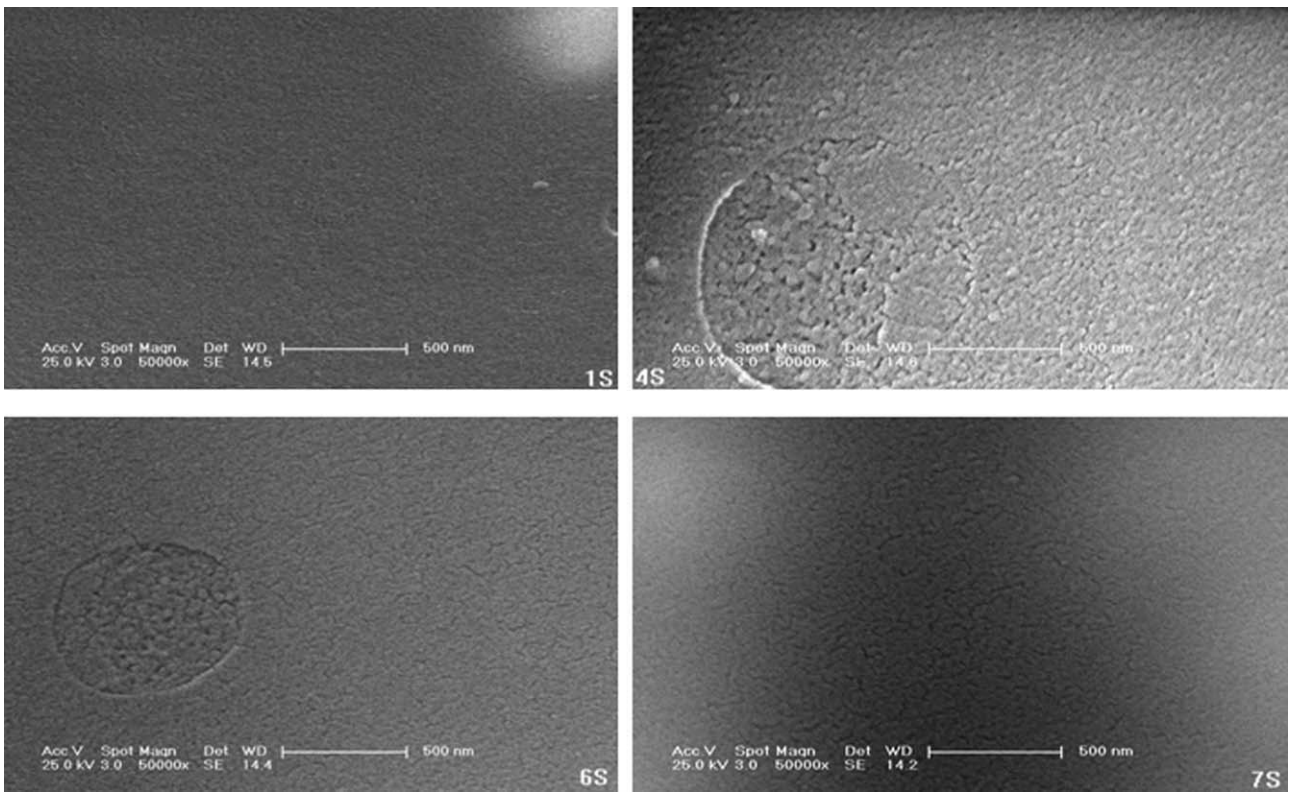

Figure 4 Surface micrographs of membranes with 10 wt % Fe_3O_4 (1S), 40 wt % Fe_3O_4 (4S), 60 wt % Fe_3O_4 (6S), and 70 wt % Fe_3O_4 (7S).

of Fe_3O_4 content. However, the pure water flux of membranes abruptly increases from 19.3 to 68.6 L m^{-2} h^{-1} when the Fe_3O_4 content is changed from 50 to 70 wt %. Our results are in accordance with those of literatures.[11,18] The pure water flux of PSF–Fe_3O_4 membranes abruptly increased from 35.9 to 208.2 L m^{-2} h^{-1} (Table II) when the Fe_3O_4 content was changed from 47.4 to 58.3 wt %, and there were no obvious corresponding differences in the surface porosity and pore dimensions of the skin of the membranes with 47.4 and 58.3 wt % Fe_3O_4.[18] Genné et al.[11] also found that the PSF–ZrO_2 (zirconia) membrane permeability was better with increased concentrations of inorganic ZrO_2 grains. Moreover, the membrane permeability was very low with concentrations below 40 wt % ZrO_2 and sharply increased with concentrations over 40 wt % ZrO_2. Their image analysis of the surface micrographs did not reveal corresponding changes in the surface porosity and pore dimensions of the skin. The authors attributed the observed flux behavior to disturbance of the normal phase inversion process because of the presence of the inorganic grains. Figure 4 illustrates the surface micrographs of some membranes. Membranes with less than 30 wt % Fe_3O_4 have a close surface porosity and pore dimension (similar to photograph 1S of Fig. 4). The membrane with 40 wt % Fe_3O_4 has bigger pore sizes and a higher surface porosity when compared with the membrane with 10 wt % Fe_3O_4 (seen in photographs 1S and 4S of Fig. 4). The change of pure water flux of membranes from 30 to 40 wt % Fe_3O_4 may result from the changes of pore size and surface porosity. However, there is no obvious difference in the surface porosity and pore dimensions of the membranes with more than 40 wt % Fe_3O_4 (seen in photographs 4S to 7S of Fig. 4). Hence, the change of pure water flux for these membranes cannot be attributed to any changes of pore size or surface porosity. There are two factors responsible for the change of flux: the surface roughness and the cross-sectional structure. The close surface roughness and similar cross-sectional structure result in a similar pure water flux for membranes with 40 and 50 wt % Fe_3O_4. However, an obvious increase of surface roughness can be found when the Fe_3O_4 content reaches 60 wt % (like micrograph 7S in Fig. 3). In addition, there are some traces remaining of macrovoids from the surface layer to the sublayer (seen in photographs 6A and 7A of Fig. 2), which can reduce the resistance of permeation from the surface to the sublayer. Furthermore, the macrovoids in the sublayer along the direction of the magnetic field can also reduce the resistance of permeation in the sublayer (Fig. 2). Both changes, the surface roughness and the cross-sectional structure, resulted in a sharp increase in water flux for membranes with over 50 wt % Fe_3O_4.

Table II shows that the initial rejection has an irregular change with the increase of Fe_3O_4 content. When the Fe_3O_4 content is below 30 wt %, the Fe_3O_4 content is low and the effect of the magnetic field can be ignored. As the Fe_3O_4 concentration is changed from 20 to 30 wt %, the change trend of initial rejection is similar to PSF–Fe_3O_4 membranes without the additional magnetic field.[18] When the Fe_3O_4 content reaches 40 wt %, the surface pore sizes become bigger (Fig. 4). Therefore, the rejection of the membrane with 40 wt % Fe_3O_4 is lower than that of the membrane with 30 wt % Fe_3O_4. The discrepancy of surface pore sizes from those membranes with 40 to 70 wt % Fe_3O_4 cannot be obtained in Figure 4 because of the resolution limit of SEM, but some round defects with few bigger pores still can be found on those skin surfaces of membranes with 40 to 60 wt % Fe_3O_4. Yang et al.[15] found that more filler enhanced the formation of larger pores and resulted in a bimodal pore distribution even though membranes with a near mean pore size of 8.9–11.5 nm. As seen in 4C and 6C photographs of Figure 4, the membranes with 40 to 60 wt % Fe_3O_4 have some bigger pores existing in round defects of the skin surfaces. The change of cross-sectional structure shall be responsible for the lowest rejection of the membrane with 50 wt % Fe_3O_4. The membrane with 50 wt % Fe_3O_4 still has a lot of finger-like macrovoids observed in the 5C photograph of Figure 3, and the membrane with 60 wt % Fe_3O_4 has few finger-like macrovoids observed in the 6C photograph of Figure 3. A few bigger pores on the skin surface of the membrane with 50 wt % Fe_3O_4 may link up with the macrovoids in the sublayer, which decreases the rejection.

Table II also shows the rejection of membranes after an antipressure test. Usually, the rejection of a membrane increases after the filtration of BSA aqueous solution because of the membrane fouling.[18] However, the rejection decrease of a membrane may be the result of an antipressure test, because a higher pressure can lead to some pinholes or mechanical failure of a membrane. The result indicates that the membrane with 70 wt % Fe_3O_4 has a good antipressure ability.

Table II shows that the initial pure water flux of a membrane in this work is lower than that of a membrane with similar Fe_3O_4 content in Ref. 18. On the contrary, the initial rejection of a membrane in this work is higher than that of a membrane with similar Fe_3O_4 content in Ref. 18. The casting solution with a higher polymer content in this work may result in smaller pore sizes and thicker skin layer, and hence a lower membrane flux and a higher rejection.

Figure 5 shows the pure water flux of a membrane versus pressure. The pure water flux after the filtration of BSA aqueous solution can reflect the absolute antifouling ability of a membrane. Data at 0.10 MPa (J_1,

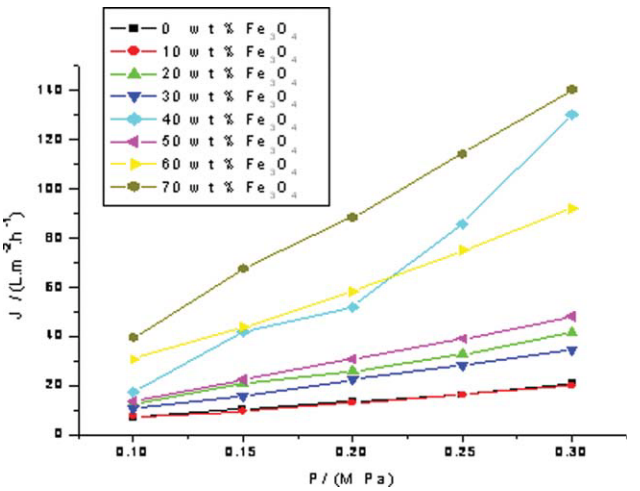

Figure 5 Flux through a membrane versus pressure. [Color figure can be viewed in the online issue, which is available at www.interscience.wiley.com.]

Table II) illustrate that the membrane with 70 wt % Fe_3O_4 has the highest pure water flux after the filtration of BSA aqueous solution. This result indicates that the membrane with 70 wt % Fe_3O_4 has the best absolute antifouling ability. The relative flux (J_r) is usually used for the comparison of membrane-relative antifouling performance[27,28] as initial molecular weight cutoff and pure water flux of membranes are different. The membrane with 70 wt % Fe_3O_4 has the lowest relative flux (Table II), and this result indicates that the membrane with 70 wt % Fe_3O_4 has the worst relative antifouling ability. Table II also shows that the relative flux of a membrane except the membrane with 70 wt % Fe_3O_4 in this work is higher than that of a membrane with similar Fe_3O_4 content in Ref. 18. This result may be relative to the pore size and its distribution of a membrane, as a big pore size and a broad pore size distribution may result in the serious blockage in a pore. Moreover, a high surface roughness (narrow grooves on the surface) of the membrane with 70 wt % Fe_3O_4 in this work may result in the removing difficulty of adhering BSA molecules. In addition, there is a normal linear relationship between the pure water flux and the pressure apart from the membrane with 40 wt % Fe_3O_4 (Fig. 5). This particular membrane may generate some defects as the pressure reaches 0.20 MPa.

CONCLUSIONS

PSF–Fe_3O_4 UF membranes with different Fe_3O_4 content were prepared in a parallel magnetic field from suspensions using the phase inversion process. In this way, magnetic Fe_3O_4 particles in a casting solution were arranged along the direction of the magnetic field during the membrane formation. This kind of oriented arrangement gradually changed the

cross-sectional microstructure of a membrane from finger-like macrovoids perpendicular to the membrane surface into macrovoids parallel to the membrane surface, with increasing Fe_3O_4 content. As a result, a novel membrane with "lamellar macrovoids" in the sublayer was prepared when the Fe_3O_4 concentration reached 70 wt %. Furthermore, the membrane with 70 wt % Fe_3O_4 not only had the best flux and rejection but also had a good antipressure ability. The obtained results may give insight to the development of novel UF membrane with excellent performance.

References

1. Rahimpour, A.; Madaeni, S. S.; Mansourpanah, Y. J Membr Sci 2007, 296, 110.
2. Chakrabarty, B.; Ghoshal, A. K.; Purkait, M. K. J Membr Sci 2008, 315, 36.
3. Witte, P.; Dijkstra, P. J.; Berg, J. W. A.; Feijen, J. J Membr Sci 1996, 117, 1.
4. Mosqueda-Jimenez, D. B.; Narbaitz, R. M.; Matsuura, T.; Chowdhury, G.; Pleizier, G.; Santerre, J. P. J Membr Sci 2004, 231, 209.
5. Pekny, M. R.; Zartman, J.; Krantz, W. B.; Greenberg, A. R.; Todd, P. J Membr Sci 2003, 211, 71.
6. Wang, D. M.; Lin, F. C.; Wu, T. T.; Lai, J. Y. J Membr Sci 1998, 142, 191.
7. Persson, K. M.; Gekas, V.; Trägârdh, G. J Membr Sci 1995, 100, 155.
8. Bohonak, D. M.; Zydney, A. L. J Membr Sci 2005, 254, 71.
9. Kallioinen, M.; Pekkarinen, M.; Mänttäri, M.; Nuortila-Jokinen, J.; Nyström, M. J Membr Sci 2007, 294, 93.
10. Doyen, W.; Adriansens, W.; Molenberghs, B.; Leysen, R. J Membr Sci 1996, 113, 247.
11. Genné, I.; Kuypers, S.; Leysen, R. J Membr Sci 1996, 113, 343.
12. Aerts, P.; Van Hoof, E.; Leysen, R.; Vankelecom, I. F. J.; Jacobs, P. A. J Membr Sci 2000, 176, 63.
13. Aerts, P.; Genne, I.; Kuypers, S.; Leysen, R.; Vankelecom, I. F. J.; Jacobs, P. A. J Membr Sci 2000, 178, 1.
14. Yang, Y. N.; Wang, P. Polymer 2006, 47, 2683.
15. Yang, Y. N.; Zhang, H. X.; Wang, P.; Zheng, Q. Z.; Li, J. J Membr Sci 2007, 288, 231.
16. Yang, Y. N.; Wu, J.; Zheng, Q. Z.; Chen, X. S.; Zhang, H. X. J Membr Sci 2008, 311, 200.
17. Jian, P.; Yahui, H.; Yang, W.; Linlin, L. J Membr Sci 2006, 284, 9.
18. Huang, Z. Q.; Chen, K.; Yin, X. T.; Zhang, Z.; Xu, H. T. J Membr Sci 2008, 315, 164.
19. Huang, Z. Q.; Guo, X. P.; Guo, C. L.; Zhang, Z. Bioprocess Biosyst Eng 2006, 28, 415.
20. Huang, Z. Q.; Chen, Z. Y.; Guo, X. P.; Zhang, Z.; Guo, C. L. Ind Eng Chem Res 2006, 45, 7905.
21. Teng, M. S.; Lin, S. H.; Wu, C. Y.; Juang, R. S. J Membr Sci 2006, 281, 103.
22. Cui, Z. China Particuology 2005, 6, 343.
23. Mulder, M. Basic Principles of Membrane Technology; Kluwer Academic Publishers: Dordrecht, 1997.
24. Mckelvey, S. A.; Koros, W. J. J Membr Sci 1996, 112, 29.
25. McHugh, A. J.; Tsay, C. S. J Appl Polym Sci 1992, 46, 2011.
26. Smolders, C. A.; Reuvers, A. J.; Boom, R. M.; Wienk, I. M. J Membr Sci 1992, 73, 259.
27. Qin, J. J.; Cao, Y. M.; Li, Y. Q.; Li, Y.; Oo, M. H.; Lee, H. Sep Purif Technol 2004, 36, 149.
28. Babu, P. R.; Gaikar, V. G. Sep Purif Technol 2001, 24, 23.